Biochemical and Biophysical Research Communications 446 (2014) 98–104

Contents lists available at ScienceDirect

Biochemical and Biophysical Research Communications

journal homepage: www.elsevier.com/locate/ybbrc

Effects of miR-31 on the osteogenesis of human mesenchymal stem cells

Qing Xie [1], Zi Wang [1], Xiaoping Bi, Huifang Zhou, Yefei Wang, Ping Gu *, Xianqun Fan *

Department of Ophthalmology, Ninth People's Hospital, Shanghai Jiao Tong University School of Medicine, Shanghai, China

ARTICLE INFO

Article history:
Received 9 February 2014
Available online 21 February 2014

Keywords:
Human mesenchymal stem cells (hMSCs)
miR-31
SATB2
Osteogenesis

ABSTRACT

Exploring the molecular mechanisms that regulate the osteogenesis of human mesenchymal stem cells (hMSCs) will bring us more efficient methods for improving the treatment of bone-related diseases. In this study, we analyzed the effects of miR-31 on the osteogenesis of hMSCs. The overexpression of miR-31 repressed the osteogenesis of hMSCs, whereas the downregulation enhanced this process. SATB2 was testified to be a direct target of miR-31, and its effects on the osteogenesis were also described. Most importantly, the knockdown of SATB2 attenuated miR-31's osteogenic effects. Taken together, our findings suggest that miR-31 regulates the osteogenesis of hMSCs by targeting SATB2.

1. Introduction

Mesenchymal stem cells (MSCs) have been reported to have the ability to differentiate into bone, cartilage and fat under appropriate induction conditions [1–3]. Since MSCs demonstrate strong regenerative properties and multi-potentiality, they have been proposed as promising candidates for cell therapies and tissue engineering. Studies employing MSCs derived from different sources [4–6] have envisioned promising future for the treatments of diseases such as myocardial infarction, spinal cord injury and graft-versus-host disease [7–9]. In reconstructive medicine, MSCs have attracted considerable interest due to their potentials to behave as excellent seed cells in tissue regeneration [10,11].

microRNAs are a class of endogenous non-coding single-strand RNA molecules of approximately 22 nucleotides in length, which incompletely complementarily bind to the 3′-UTR of target mRNAs and inhibit the process of translation [12,13]. miRNAs have emerged as important regulators of diverse physiological and pathological processes, recent studies have revealed several microRNAs that regulate the osteogenesis of MSCs, miR-182 represses the osteogenesis of MSCs by targeting FoxO1 [14], miR-34 inhibits the osteoblast proliferation and differentiation of mouse by targeting SATB2 [15] and miR-100 regulates human adipose-derived mesenchymal stem cells (hASCs) by affecting BMPR-2 [16].

In this study, we analyzed miR-31's effects on osteogenesis of hMSCs by transfecting exogenous plasmids expressing miR-31 or miR-31 inhibitors into hMSCs and our data demonstrated that miR-31 regulated the osteogenesis of hMSCs by targeting SATB2.

2. Methods and materials

2.1. Cell culture

hMSCs were purchased from Cyagen Biosciences Inc. (Guangzhou, China) as previously described [17]. Next, hMSCs were cultured in DMEM/F12 (Invitrogen, Carlsbad, CA) supplemented with 10% FBS (Invitrogen) and 100 units/ml penicillin and streptomycin (Invitrogen) and incubated at 37 °C and a 5% CO_2 humid atmosphere, cells from passage 2 were used for the following experiments.

2.2. Reverse transcription and quantitative polymerase chain reaction (qPCR)

Total RNA was extracted from each sample using the RNeasy Mini Kit (Qiagen, Valencia, CA) and first-strand complementary cDNA was synthesized using a PrimeScript™ RT reagent kit (Perfect Real Time, TaKaRa, Dalian, China) [18]. The resulting cDNAs were diluted 20-fold in nuclease-free water (Invitrogen) and were used as templates for qPCR. qPCR was carried out in a 20-μl solution containing 10 μl reaction mixture, 2 μl of cDNA, and 300 nM of gene-specific primers designed using Primer 3 software. The primer sequences used in this study were listed in Table 1. The qPCR was conducted using a 7500 Real-Time PCR Detection System (Applied Biosystems, Irvine, CA) and activated at 95 °C for 10 min and 40 cycles of amplification (15 s at 95 °C and 1 min at 60 °C). The efficiency of the reaction was measured with primers using

* Corresponding authors. Address: Department of Ophthalmology, Ninth People's Hospital, Shanghai Jiao Tong University School of Medicine, Shanghai 200011, China. Fax: +86 021 6313 7148.

E-mail addresses: guping2009@hotmail.com (P. Gu), fanxq@sh163.net (X. Fan).

[1] These authors contributed equally to this work.

http://dx.doi.org/10.1016/j.bbrc.2014.02.058
0006-291X/

Table 1
Primers used for qPCR.

Genes	Accession No.	Forward (5′-3′)	Reverse (5′-3′)	Annealing temperature (°C)	Product size (base pairs)
SATB2	NM_001172509	gcagttggacggctctctt	caccttcccagcttgattattcc	60	168
Runx2	NM_001015010	tggttactgtcatggcgggta	tctcagatcgttgaaccttgcta	60	101
BSP	NM_004967	cactggagccaatgcagaaga	tggtggggttgtaggttcaaa	60	106
Ocn	NM_199173	cactcctcgccctattggc	ccctcctgcttggacacaaag	60	112
Osx	NM_152860	cctctgcgggactcaacaac	agcccattagtgcttgtaaagg	60	128
GAPDH	NM_001256799	ggagcgagatccctccaaaat	ggctgttgtcatacttctcatgg	60	197

serial dilutions of the cDNA (1:1, 1:5, 1:25, 1:125, 1:625 and 1:3125). For miR-31, qPCR was conducted by using an EzOmics™ miRNA qPCR Detection Primer Set (Biomics Biotechnologies Co., Ltd.). Each sample was tested in triplicate. The relative gene expression levels of mRNA and miRNA were analyzed using the Pfaffl method [19] in which GADPH and U6 were used as endogenous normalization controls.

2.3. Plasmids construction

The plasmid expressing hsa-miR-31 was constructed and termed as miR-31. Total RNA was extracted from hMSCs and then cDNA was generated by RT-PCR. The target amplicon was generated using the primer: forward gtatgagaccactcggatcggaaaagtaaaacact gaagagtc, reverse agcggtttaaacttaagctaaaaaatgtcatggaaatccacatcc. Next, the PCR product was cloned into the pH1-GFP vector between the BamHI and HindIII (Promega Biotech Co., Ltd., China). The plasmid expressing the reverse complementary sequence of hsa-miR-31 was termed as miR-31 inhibitor, the constructed sequence was synthesized by GeneChem (GeneChem Technology Co., Ltd, China) as listed in Table 2, and then cloned into pU6-GFP vector between BamHI and HindIII (Promega). The SATB2 expressing plasmid was termed as p-SATB2, the target sequence was generated by RT-PCR using the primer: forward agtcgctagcatggagcggcggagcgagag, reverse cgggtaccggtggtctctggtcaatttcggcagg and then cloned into pCMV-GFP vector between the NheI and AgeI (Promega). The fragments of the SATB2 3′-UTR (NM_001172509) containing the predicted binding site of hsa-miR-31 and its mutant sequence were synthesized by GeneChem as listed in Table 2, and then cloned downstream of the luciferase sequence in between the XbaI cleavage sites of the pGL3-control vector (Promega). The constructed plasmids were respectively termed as SATB2-3′-UTR-wt (position 2376–2383 of SATB2 3′-UTR, wild type) and SATB2-3′-UTR-mut (position 2376–2383 of SATB2 3′-UTR, mutant). The pRL-TK vector containing the renilla luciferase reporter gene was obtained directly from Promega.

Table 2
Constructed sequences used in this study.

Name	Forward (5′-3′)
miR-31 inhibitor	agctaaaaaaggcaagatgctggcatagct ggatccagctatgccagcat cttgccttttttt
SATB2-3′-UTR wild type	gctctagaaatttcactgccaagtttgcagtgg ttctaagtgaatctgtgg gcattttagcctgtgg**tcttgcca**gatctttgcgaatta caatgcatatatgtctattta ttcaatatctgtcatataatatctatttgga agaagaaactttctcttgtagtgcctct tgacaatctagagc
SATB2-3′-UTR mutant	gctctagaaatttcactgccaagtt tgcagtggttctaagtg aatctgtgggcattttagcctgtgg**gaggcaat** gatctttgcgaattaca atgcatatatgtctatttattcaatatctgtcat ataatatctatttgga agaagaaactttctcttgtagtgcctct tgacaatctagagc

2.4. Plasmids and siRNA transfection

The small interfering RNA of SATB2 was designed and synthesized by Biomics Biotechnologies, sense: 5′-gcuuaguccacaacuuguadtdt-3′, antisense: 5′-uacaaguuguggacuaagcdtdt-3′. hMSCs were seeded in 6-well plates at a density of 4×10^5 cells/well before transfection. The transfection was conducted in Opti-MEM (Invitrogen), and the transfection mix was composed of 3 μg of plasmid and optimal volume of Lipofectamine 2000 Reagent (Invitrogen). The siRNA was transfected into the hMSCs at a final concentration of 100 nM. The medium was changed to regular culture medium 8 h after transfection.

2.5. Western blotting analysis

We performed Western blotting analysis according to a standard protocol as previously described [16]. Confluent hMSCs were lysed with RIPA lysis buffer (Beyotime Institute of Biotechnology, China) supplemented with PMSF (Invitrogen), protein contents were determined using a BCA protein assay kit (Thermo Fisher Scientific Inc., Waltham, MA). Next, the total proteins were separated by 10% SDS–PAGE and electro-blotted onto a PVDF membrane (Millipore Corporation, Billerica, MA). The membranes were then incubated with an optimal concentration of the primary antibodies: anti-osteocalcin, anti-SATB2, anti-BSP and anti-β-actin (Abcam, Cambridge, MA). Immunoreactive bands were detected with anti-rabbit or anti-mouse fluorescein-conjugated secondary antibody (Abcam) and visualized by Odyssey V3.0 image scanning.

2.6. ALP, ARS staining and quantitative ALP assay

hMSCs were cultured in a 12-well plate, washed twice with PBS and fixed in 4% polyoxymethylene for 10 min. ALP staining was performed with a BCIP/NBT Alkaline Phosphatase Color Development Kit (Beyotime) according to the manufacturer's instructions. Alizarin red S staining solution was obtained from Sigma as previously described [20]. hMSCs were first washed with PBS and fixed in cold 95% (v/v) ethanol for 1 h, then fixed hMSCs were incubated with staining solution at 37 °C for 30 min. For quantitative ALP measurements, hMSCs were lysed using RIPA lysis buffer (Beyotime), the cell supernatant was collected into a 96-well plate. Next, substrates and p-nitrophenol from Alkaline Phosphatase Assay Kit (Beyotime) were subsequently added and incubated for 10 min at 37 °C. Finally, the ALP activity was determined at the wavelength of 405 nm.

2.7. Dual luciferase reporter assay

0.4 μg of pGL3-control plasmid, 0.3 μg of pRL-TK plasmid and 0.3 μg of pH1-GFP plasmid were co-transfected into 293T cells using Lipofectamine 2000 Reagent (Invitrogen). Cells were har-

vested 48 h after transfection and assayed for firefly and renilla luciferase activity using the Dual-Glo™ Luciferase Assay System (Promega). Firefly luciferase activity was normalized to renilla luciferase activity.

2.8. Statistical analysis

The results represent the average of three independent experiments, and the data are presented as the mean ± SD. Statistical significance was determined using the unpaired Student's *t*-test, and a value of $^{*}P < 0.05$ was considered to be statistically significant.

2.9. Bio-information prediction

To predict the target genes of hsa-miR-31 during the osteoblast differentiation of hMSCs, we selected three scientifically sanctioned miRNA target prediction databases: TargetScan (http://www.targetscan.org), PicTar (http://www.pictar.org), and miRbase (http://www.mirbase.org).

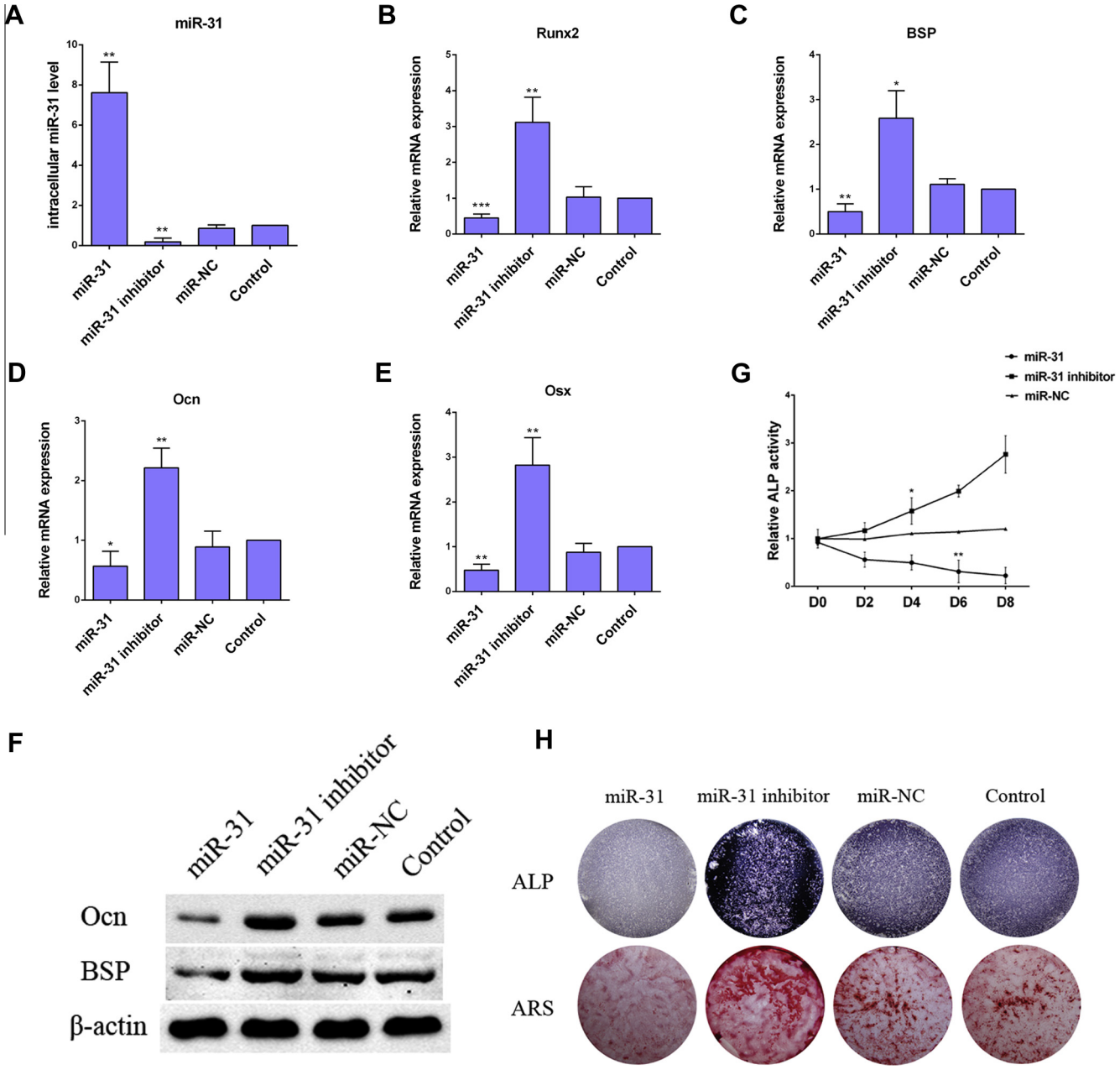

Fig. 1. miR-31 inhibited osteoblast differentiation, whereas the miR-31 inhibitor enhanced the osteogenesis of hMSCs. qPCR detected intracellular miR-31 levels after transfection with exogenous plasmids expressing miR-31, a miR-31 inhibitor and the negative control (A); these data were normalized to U6 as a control. qPCR detection of osteogenic specific genes including Runx2 (B), BSP (C), Ocn (D) and Osx (E) showed that miR-31 reduced hMSC osteogenesis by over 50%, but the miR-31 inhibitor increased the osteogenesis by more than 1.5-fold. These data are the averages of three independent experiments and were all normalized to GADPH. All the qPCR data are averages of three independent experiments, $^{*}P < 0.05$, $^{**}P < 0.01$, $^{***}P < 0.001$. Western blot analyses indicated that Ocn and BSP were repressed by miR-31 overexpression, whereas their expression was enhanced by the miR-31 inhibitor (F). ALP and ARS staining revealed that the exogenous overexpression of miR-31 reduced the ALP level and the amount of calcium deposits in hMSCs, whereas the miR-31 inhibitor elevated these levels (G). A quantitative ALP assay indicated that ALP activity was inhibited by miR-31–27% of the control group activity on day 6 but was elevated to 2.4-fold higher than the control group by the miR-31 inhibitor on day 4 (H). Data from each time point were each normalized to the negative control group, and these data were averages of three independent experiments, $^{*}P < 0.05$, $^{**}P < 0.01$.

3. Results

3.1. miR-31 inhibited osteoblast differentiation whereas the miR-31 inhibitor enhanced hMSC osteogenesis

qPCR analyzed the intracellular miR-31 content after the transfection of exogenous plasmids expressing miR-31, the miR-31 inhibitor and the empty pCMV-GFP vector, termed as miR-31, miR-31 inhibitor and miR-NC, respectively. The intracellular miR-31 level was found to be elevated dramatically by miR-31 transfection, whereas the miR-31 inhibitor led to reduced miR-31 content, miR-NC had hardly any effect on miR-31 content (Fig. 1A). Western blot analysis indicated that Ocn and BSP were both repressed by transfection with miR-31, but the downregulation of miR-31 by transfecting the miR-31 inhibitor increased Ocn and BSP expression levels; the negative control had no effect on their expression levels (Fig. 1B). qPCR was used to detect the mRNA expression levels of some osteoblast specific genes, including Runx2, BSP, Ocn and Osx. These data indicated that the exogenous overexpression of miR-31 reduced Runx2 (Fig. 1C), BSP (Fig. 1D), Ocn (Fig. 1E) and Osx (Fig. 1F) expression levels by over 50%, whereas the miR-31 inhibitor elevated levels by more than 1.5-fold, the negative control had no effect. ALP and ARS staining also demonstrated that the ALP level and calcium deposition in miR-31-transfected hMSCs were significantly lower than those in the negative control and untreated hMSCs. On the contrary, these levels were much higher in the miR-31 inhibitor-transfected hMSCs (Fig. 1G). The quantitative ALP assay performed at different time points after transfection with miR-31, the miR-31 inhibitor and miR-NC implied that ALP activity was inhibited by 27% of the control group on day 6 after miR-31 transfection. The miR-31 inhibitor could enhance ALP levels to 2.4-fold higher than that of the control group (miR-NC) (Fig. 1H). In conclusion, the above results indicated that the overexpression of miR-31 can repress hMSC osteogenesis, but the downregulation of miR-31 could potentiate the osteoblastic features of hMSCs.

3.2. The 3′-UTR of SATB2 mRNA is a direct target of miR-31

The plasmids expressing miR-31, miR-31 inhibitor and the negative control were individually transfected into hMSCs. qPCR analysis implied that SATB2 mRNA levels did not change significantly in different transfection groups (Fig. 2A). However, the SATB2 protein level was repressed by miR-31, and promoted by the miR-31 inhibitor when compared with the negative control and untreated hMSCs (Fig. 2B). As shown in Fig. 2C, the predicted binding sites of hsa-miR-31 is located at position 2376–2383 of the 3′-UTR of SATB2's mRNA. To verify the predicted binding sites, the firefly luciferase reporter system containing the wild type miR-31 binding site and its mutant sequence was constructed and co-transfected with the miR-31 overexpression plasmid and the negative control, along with renilla luciferase reporter system as a normalizer. As Fig. 2D shows, the luciferase activity assay detected that the co-transfection of miR-31 overexpression plasmid (miR-31) and the wild type 3′-UTR binding site (SATB2-3′-UTR-wt) decreased the luciferase expression level compared with the miR-31 negative control (miR-NC). Furthermore, the co-transfection of miR-31 and the mutant 3′-UTR binding site (SATB2-3′-

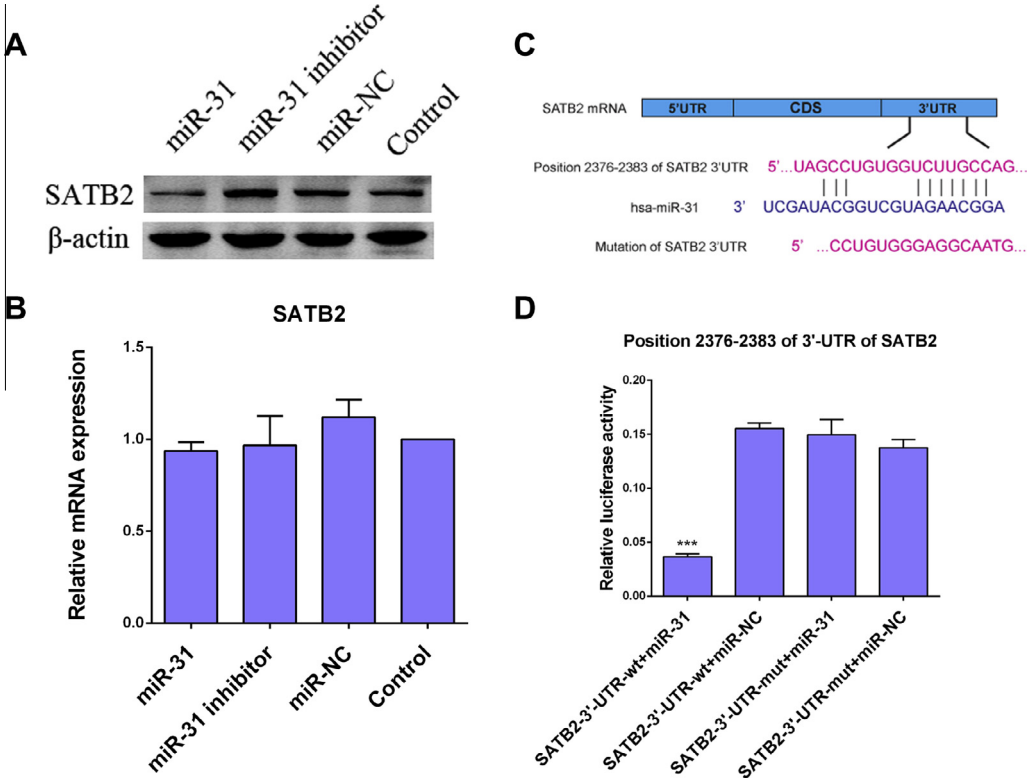

Fig. 2. The 3′-UTR of SATB2 mRNA is a direct target of miR-31. Western blot analysis indicated that the SATB2 expression level was inhibited by the overexpression of miR-31, but the downregulation of miR-31 via the transfection of the miR-31 inhibitor promoted its expression (A). qPCR showed that neither exogenous miR-31 nor the miR-31 inhibitor had special effects on SATB2 mRNA levels (B). Position 2376–2383 of the 3′-UTR of SATB2's mRNA and its mutation sequence we designed (C) showed that miR-31 may directly target the 3′-UTR of SATB2 mRNA and interfere with SATB2 protein synthesis. The dual luciferase reporter system indicated that the co-transfection of miR-31 and its wild type 3′-UTR binding site, termed as SATB2-3′UTR-wt, dramatically reduced luciferase activity, whereas miR-31 had no effects on the mutated 3′-UTR binding region (SATB2-3′UTR-mut) (D). All of these data were averages from three independent experiments, and the firefly luciferase activity data were all normalized to renilla luciferase activity as a control, $^{***}P < 0.001$.

UTR-mut) seemed to have no effect on luciferase levels. Considering all of the results, we observed that the miR-31 expression level seemed to have a negative correlation with the SATB2 protein level. Next, we conducted the exogenous transfection of miR-31 and miR-31 and found that the overexpression of miR-31 could repress the SATB2 protein level, whereas the knockdown of miR-31 could elevate it. Neither of these constructs affected SATB2 mRNA levels. We finally determined via the dual luciferase reporter system that the 3′-UTR at position 2376–2383 of the SATB2 is the direct target of miR-31. In short, our results demonstrated that SATB2 mRNA is a direct target of miR-31.

3.3. Overexpression of SATB2 promotes osteogenic differentiation whereas the knockdown of SATB2 impairs hMSC osteogenesis

To determine what effects SATB2 may have on the osteogenesis, we transfected the SATB2 overexpression plasmid (p-SATB2) and small interfering RNA (si-SATB2) into hMSCs (Fig. 3A). qPCR results indicated that the SATB2 mRNA expression level was increased by over sevenfold after transfection with p-SATB2, whereas the transfection of si-SATB2 decreased the SATB2 mRNA level by more than 70% when compared with the negative control. The results of Western blot analysis were consistent with qPCR, showing that SATB2 protein levels were increased by p-SATB2, whereas they were decreased by si-SATB2 when compared with the negative control (Fig. 3B). Interestingly, we also found that the overexpression of SATB2 resulted in increased mRNA expression levels of osteoblast-specific genes, such as Runx2 (Fig. 3C), BSP (Fig. 3D), Ocn (Fig. 3E) and Osx (Fig. 3F), by over 150%, In contrast, the SATB2-knockdown hMSCs exhibited a reduced potential to become osteoblasts because mRNA expression levels of osteogenic related genes declined by more than 50% compared with the negative control group. Protein expression levels such as Ocn and BSP were similarly increased by transfection with p-SATB2, whereas they decreased significantly upon transfection with si-SATB2 compared with the untreated control hMSCs (Fig. 3G). The ALP level and the amount of calcium deposition were also assessed after performing ALP and ARS staining, indicating that SATB2-overexpressing hMSCs could generate more ALP and more calcium deposition, whereas the SATB2 knockdown hMSCs were much less likely to differentiate into osteoblasts than the control hMSCs (Fig. 3H). Taken together, we suggest that SATB2 is a critical regulator of osteogenesis and that the overexpression of SATB2 promotes osteoblast differentiation, whereas the knockdown of SATB2 impairs osteogenesis.

3.4. SATB2 knockdown inhibits the effects of miR-31

To verify the relationship between miR-31 and SATB2 further, we co-transfected the miR-31 inhibitor, which has previously been shown to promote hMSC osteogenesis, and si-SATB2 into hMSCs. Next, qPCR, Western blotting, and ALP and ARS staining were

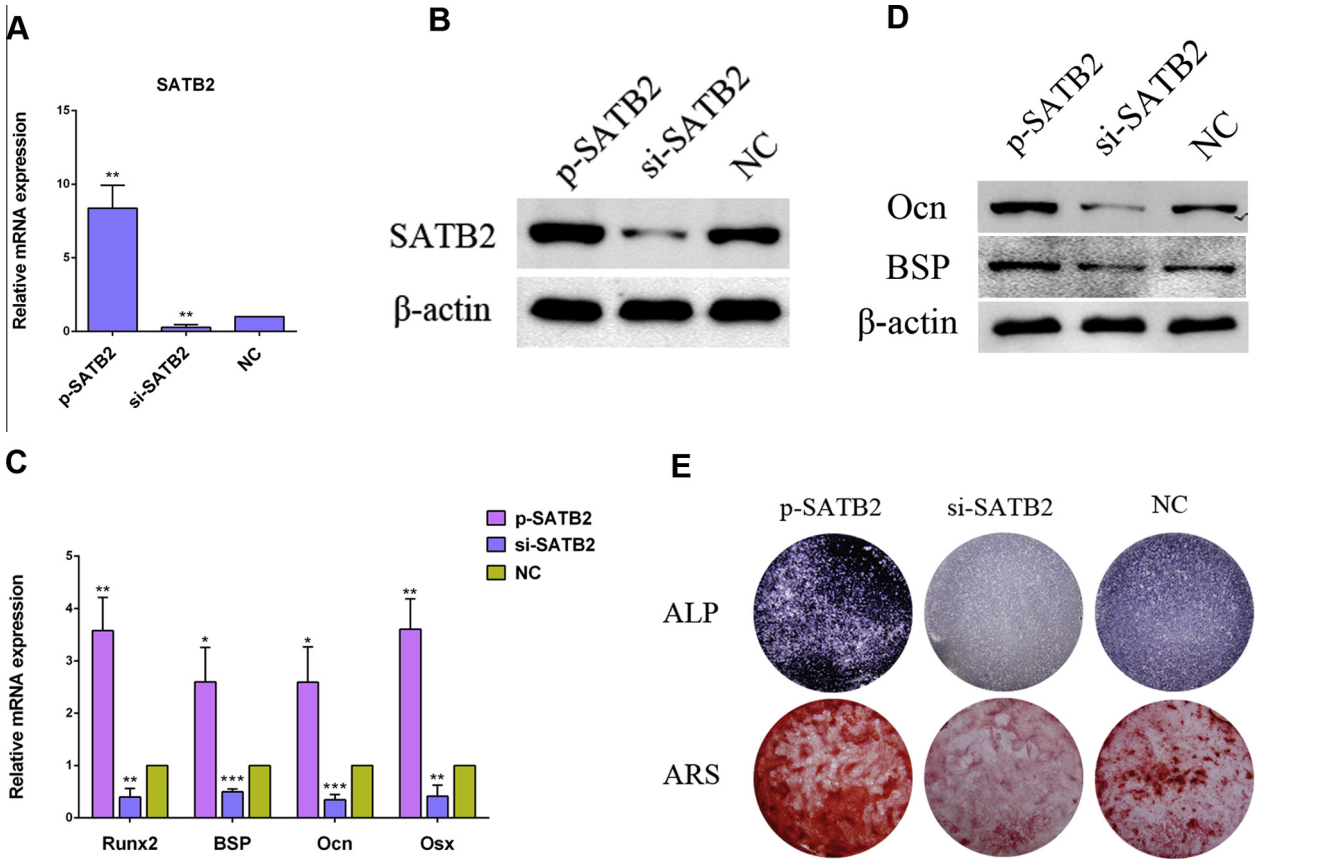

Fig. 3. The overexpression of SATB2 promotes osteogenic differentiation, whereas the knockdown of SATB2 impairs hMSC osteogenesis. qPCR revealed that the transfection of the SATB2 overexpression plasmid, termed p-SATB2, increased the SATB2 mRNA level by more than 7-fold, whereas the transfection of small interfering RNA designed for SATB2 mRNA, termed si-SATB2, decreased SATB2 mRNA level by over 70% (A). Western blotting also revealed that SATB2 protein levels were elevated by the transfection of p-SATB2 while they were diminished by si-SATB2 (B). Expression levels of osteoblast specific marker genes including Runx2, BSP, Ocn and Osx were elevated by the transfection of p-SATB2 by over 150% but repressed by si-SATB2 to levels less than 50% of the control (C). The expression levels of osteogenic specific proteins including Ocn and BSP were elevated by p-SATB2 but repressed by si-SATB2 (D). Intracellular ALP levels and calcium deposit levels were detected by ALP and ARS staining, respectively (E). These levels were increased by transfection with p-SATB2 but were decreased by si-SATB2. All of these data were averages of three independent experiments, qPCR data were normalized to GADPH, $^{*}P < 0.05$, $^{**}P < 0.01$, $^{***}P < 0.001$.

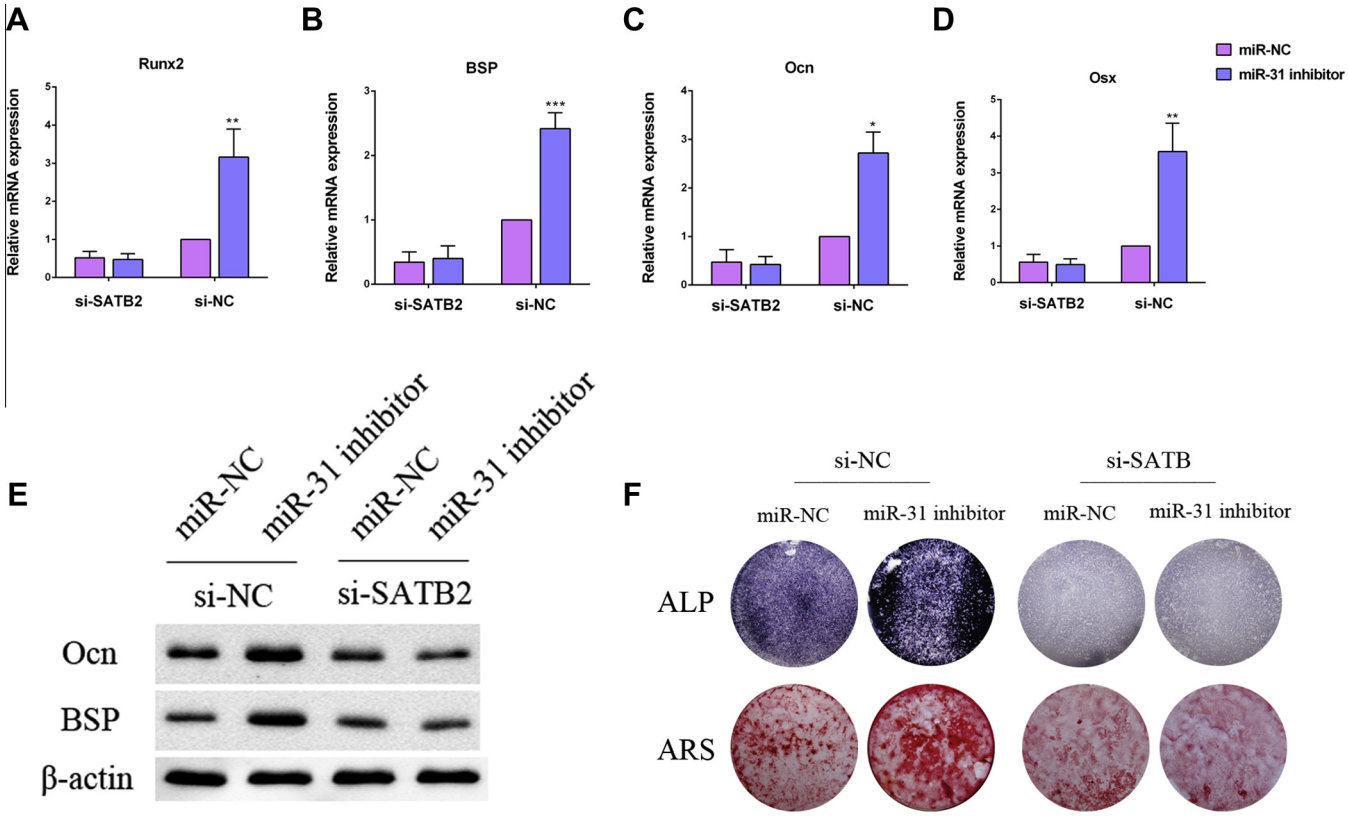

Fig. 4. The knockdown of SATB2 attenuates the effects of miR-31 inhibitor. qPCR detected that mRNA expression levels of osteogenic associated genes such as Runx2 (A), BSP (B), Ocn (C) and Osx (D) in SATB2 knockdown hMSCs could not be increased by transfection with the miR-31 inhibitor, but the miR-31 inhibitor could still elevate the expression levels of osteogenic related genes by over 1.5-fold in normal hMSCs. Western blot results showed that the protein expression levels of Ocn and BSP in SATB2 knockdown hMSCs could not be elevated by the miR-31 inhibitor, but increased expression could be observed by the transfection of the miR-31 inhibitor in normal hMSCs (E). Transfection of the miR-31 inhibitor enhanced normal hMSCs' intracellular ALP levels and calcium deposition as evidenced by ALP and ARS staining, but the inhibitor failed to increase levels in SATB2 knockdown hMSCs (F). All these data were averages of three independent experiments, and the qPCR data were all normalized to GADPH, $^{*}P < 0.05$, $^{**}P < 0.01$.

conducted to detect the effects of the miR-31 inhibitor in SATB2-knockdown hMSCs. As indicated, transfection of miR-31 inhibitor had no significant impact on promoting mRNA expression levels of osteogenic related genes, such as Runx2 (Fig. 4A), BSP (Fig. 4B), Ocn (Fig. 4C) and Osx (Fig. 4D), in SATB2-knockdown hMSCs compared with the negative control. However, the miR-31 inhibitor could still promote normal hMSC osteogenesis by more than 1.5-fold. Similar results are clearly shown in Fig. 4E; Ocn and BSP expression levels in SATB2-knockdown hMSCs were not increased by miR-31 inhibitor transfection compared with the negative control. Both ALP and ARS staining results indicated that the SATB2-knockdown hMSCs were not likely to be osteogenically enhanced by the miR-31 inhibitor, but normal hMSCs could be promoted to differentiate into osteoblasts as previously observed (Fig. 4F). Taken together, these results indicate that the knockdown of SATB2 inhibits miR-31's effects on the osteogenesis of hMSCs.

4. Discussion

Mesenchymal stem cells (MSC) isolated from various tissues have exhibited great potential for use in reconstructive therapy. Determining the underlying mechanisms that govern MSCs' proliferation and differentiation would provide us more effective approaches to make progress in stem cell-related therapies. Recently, miRNAs have attracted tremendous focus for their extensive regulatory function by affecting the post-transcription process of protein synthesis. In this study, we identified miR-31 as a negative regulator of osteogenic differentiation. The overexpression of miR-31 inhibited the osteogenesis of hMSCs, whereas the inhibition of miR-31 enhanced this process.

It has been reported that miR-31 is downregulated in some tumor tissues and acts as a negative regulator of tumor proliferation and metastasis [21], and our colleagues have reported that rno-miR-31 was downregulated during osteogenic induction in rat bone marrow derived MSCs [20]. In this study, we selected the hsa-miR-31 to test what effects it may have on the osteogenesis of hMSCs. Our data revealed that miR-31 transfection resulted in reduction of SATB2 protein level, whereas miR-31 inhibitor led to promotion. However, qPCR results indicated that the mRNA level of SATB2 was affected by neither miR-31 nor miR-31 inhibitor. We supposed that miR-31 might lead to translation repression of SATB2 instead of mRNA degradation. We predicted the binding sites of hsa-miR-31 using bio-information databases like PicTar, mirbase and TargetScan, and found out that SATB2 may be one of its many targets. Meanwhile, the dual luciferase reporter assay has identified SATB2 as a direct target of miR-31. According to our data, miR-31 was demonstrated to bind to position 2376–2383 of the 3′-UTR of SATB2's mRNA, which suggested that miR-31 regulated SATB2 expression by interfering with mRNA translation.

SATB2 plays a critical role in regulating osteogenesis, it has been reported to not only bind individually to the promoter of osteogenic specific genes, but also synergistically enhance the regulatory role of Runx2 [22]. Our results revealed that the overexpression of SATB2 promote the osteogenesis of hMSCs by

upregulating both mRNA and protein expression levels of osteoblast-specific genes, such as Runx2, BSP, Ocn and Osx. On the contrary, SATB2-knockdown hMSCs exhibited decreased expression levels of Runx2, BSP, Ocn and Osx. As our data demonstrated, the overexpression of miR-31 repressed the osteogenesis of hMSCs whereas the inhibition of miR-31 enhanced it. These results indicate that SATB2 may function as a bridge that connects miR-31 and the osteogenesis. To test this hypothesis, we transfected miR-31 inhibitor into SATB2-knockdown hMSCs and detected the expression levels of Runx2, BSP, Ocn and Osx. Our results demonstrated that the transfection of the miR-31 inhibitor no longer exhibited promotive effects on the osteogenesis of SATB2-knockdown hMSCs. Taken together, these data suggest that miR-31 regulates hMSC osteogenesis by directly targeting SATB2.

In conclusion, our results demonstrate that miR-31 performed as a negative regulator of the osteogenesis of hMSCs. miR-31 exhibited its regulatory function by affecting the expression level of SATB2, a critical osteogenesis-related gene, by directly binding to 3′-UTR of its mRNA. Overall, our findings suggest that miR-31 plays an important regulatory role in osteogenic differentiation and might function by targeting SATB2 directly.

Acknowledgments

This work was supported by the National Natural Science Foundation of China (31271029, 81320108010, 81170876, 81000404, 81100696, 81200720), and the Shanghai Municipality Commission for Science and Technology (12441903003).

References

[1] E.M. Fischer, P. Layrolle, C.A. Van Blitterswijk, J.D. De Bruijn, Bone formation by mesenchymal progenitor cells cultured on dense and microporous hydroxyapatite particles, Tissue Eng. 9 (2003) 1179–1188.
[2] S. Seo, K. Na, Mesenchymal stem cell-based tissue engineering for chondrogenesis, J. Biomed. Biotechnol. 2011 (2011) 806891.
[3] S. Bork, P. Horn, M. Castoldi, I. Hellwig, A.D. Ho, W. Wagner, Adipogenic differentiation of human mesenchymal stromal cells is down-regulated by microRNA-369-5p and up-regulated by microRNA-371, J. Cell. Physiol. 226 (2011) 2226–2234.
[4] J.W. Kim, S.Y. Kim, S.Y. Park, Y.M. Kim, J.M. Kim, M.H. Lee, H.M. Ryu, Mesenchymal progenitor cells in the human umbilical cord, Ann. Hematol. 83 (2004) 733–738.
[5] S.T. Richard Tuli, Sumon Nandi, Mark L. Wang, Peter G. Alexander, Hana Haleem-Smith, William J. Hozack, Paul A. Manner, Keith G. Danielson, Rocky S. Tuan, Characterization of multipotential mesenchymal progenitor cells derived from human trabecular bone, Stem Cells 21 (2003) 681–693.
[6] D.A. De Ugarte, K. Morizono, A. Elbarbary, Z. Alfonso, P.A. Zuk, M. Zhu, J.L. Dragoo, P. Ashjian, B. Thomas, P. Benhaim, I. Chen, J. Fraser, M.H. Hedrick, Comparison of multi-lineage cells from human adipose tissue and bone marrow, Cells Tissues Organs 174 (2003) 101–109.
[7] O. Ringden, M. Uzunel, I. Rasmusson, M. Remberger, B. Sundberg, H. Lonnies, H.U. Marschall, A. Dlugosz, A. Szakos, Z. Hassan, B. Omazic, J. Aschan, L. Barkholt, K. Le Blanc, Mesenchymal stem cells for treatment of therapy-resistant graft-versus-host disease, Transplantation 81 (2006) 1390–1397.
[8] P.-Y.M. Pablo Maureira, Yu Fengxu, Sylvain Poussier, Yihua Liu, Frederique Groubatch, Aude Falanga, Nguyen Tran, Repairing chronic myocardial infarction with autologous mesenchymal stem cells engineered tissue in rat promotes angiogenesis and limits ventricular remodeling, J. Biomed. Sci. 19 (2012) 93.
[9] R. Quertainmont, D. Cantinieaux, O. Botman, S. Sid, J. Schoenen, R. Franzen, Mesenchymal stem cell graft improves recovery after spinal cord injury in adult rats through neurotrophic and pro-angiogenic actions, PLoS One 7 (2012) e39500.
[10] J.Z. Li, G.R. Hankins, C. Kao, H. Li, J. Kammauff, G.A. Helm, Osteogenesis in rats induced by a novel recombinant helper-dependent bone morphogenetic protein-9 (BMP-9) adenovirus, J. Gene Med. 5 (2003) 748–756.
[11] H. Zhou, C. Xiao, Y. Wang, X. Bi, S. Ge, X. Fan, In vivo efficacy of bone marrow stromal cells coated with beta-tricalcium phosphate for the reconstruction of orbital defects in canines, Invest. Ophthalmol. Vis. Sci. 52 (2011) 1735–1741.
[12] B.J. Reinhart, F.J. Slack, M. Basson, A.E. Pasquinelli, J.C. Bettinger, A.E. Rougvie, H.R. Horvitz, G. Ruvkun, The 21-nucleotide let-7 RNA regulates developmental timing in *Caenorhabditis elegans*, Nature 403 (2000) 901–906.
[13] A.E. Pasquinelli, B.J. Reinhart, F. Slack, M.Q. Martindale, M.I. Kuroda, B. Maller, D.C. Hayward, E.E. Ball, B. Degnan, P. Muller, J. Spring, A. Srinivasan, M. Fishman, J. Finnerty, J. Corbo, M. Levine, P. Leahy, E. Davidson, G. Ruvkun, Conservation of the sequence and temporal expression of let-7 heterochronic regulatory RNA, Nature 408 (2000) 86–89.
[14] K.M. Kim, S.J. Park, S.H. Jung, E.J. Kim, G. Jogeswar, J. Ajita, Y. Rhee, C.H. Kim, S.K. Lim, MiR-182 is a negative regulator of osteoblast proliferation, differentiation, and skeletogenesis through targeting FoxO1, J. Bone Miner. Res. 27 (2012) 1669–1679.
[15] J. Wei, Y. Shi, L. Zheng, B. Zhou, H. Inose, J. Wang, X.E. Guo, R. Grosschedl, G. Karsenty, MiR-34s inhibit osteoblast proliferation and differentiation in the mouse by targeting SATB2, J. Cell Biol. 197 (2012) 509–521.
[16] Y. Zeng, X. Qu, H. Li, S. Huang, S. Wang, Q. Xu, R. Lin, Q. Han, J. Li, R.C. Zhao, MicroRNA-100 regulates osteogenic differentiation of human adipose-derived mesenchymal stem cells by targeting BMPR2, FEBS Lett. 586 (2012) 2375–2381.
[17] M. Federici, J. Qin, W.-Q. Li, L. Zhang, F. Chen, W.-H. Liang, F.F. Mao, X.-M. Zhang, B.T. Lahn, W.-H. Yu, A.P. Xiang, A stem cell-based tool for small molecule screening in adipogenesis, PLoS One 5 (2010) e13014.
[18] Y. Hu, J. Ji, J. Xia, P. Zhao, X. Fan, Z. Wang, X. Zhou, M. Luo, P. Gu, An in vitro comparison study: the effects of fetal bovine serum concentration on retinal progenitor cell multipotentiality, Neurosci. Lett. 534 (2013) 90–95.
[19] M.W. Pfaffl, A new mathematical model for relative quantification in real-time RT-PCR, Nucleic Acids Res. 29 (2001) e45.
[20] Y. Deng, S. Wu, H. Zhou, X. Bi, Y. Wang, P. Zhao, Y. Hu, P. Gu, X. Fan, Effects of a miR-31, Runx2 and Satb2 regulatory loop on the osteogenic differentiation of bone marrow mesenchymal stem cells, Stem Cells Dev. (2013).
[21] D. Hua, D. Ding, X. Han, W. Zhang, N. Zhao, G. Foltz, Q. Lan, Q. Huang, B. Lin, Human miR-31 targets radixin and inhibits migration and invasion of glioma cells, Oncol. Rep. 27 (2012) 700–706.
[22] G. Dobreva, M. Chahrour, M. Dautzenberg, L. Chirivella, B. Kanzler, I. Farinas, G. Karsenty, R. Grosschedl, SATB2 is a multifunctional determinant of craniofacial patterning and osteoblast differentiation, Cell 125 (2006) 971–986.